

Taking advantage of ortho- and peri-substitution to design original 9-membered P,O,Si-heterocycles

Thomas Delouche,^a Elsa Caytan,^a Cassandre Quinton,^a Thierry Roisnel,^a Marie Cordier,^a Vincent Dorcet,^a Muriel Hissler,^a and Pierre-Antoine Bouit^{*,a}

Univ Rennes, CNRS, ISCR - UMR 6226, F-35000 Rennes.

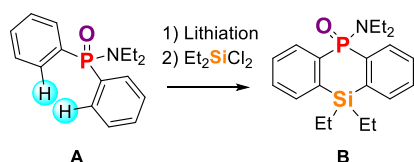
A family of 9 cyclic phosphine-disiloxane featuring peri-substituted naphthyl(Nap)/acenaphthyl(Ace) scaffolds have been prepared and fully characterized including X-ray structure, which allows a detailed structural analysis. This straightforward synthesis takes advantage of both ortho- and peri-substitution of Nap/Ace-substituted phosphine oxides. The synthetic method allows diversifying the polyaromatic platform (Nap and Ace) as well as the Si substituents (Me and Ph). Despite a strong steric congestion, the P-atom remains reactive toward oxidation or coordination. In particular, Au(I) complex could be prepared. All the compounds display absorption/luminescence in the UV-Vis range. Surprisingly, the P-trivalent derivatives display unexpected luminescence in the green in solid-state.

Introduction

Ortho-metalations (metalation in ortho position induced by the presence of a functional group) belong to the Complex-Induced Proximity Effect based reactions and are widely used in organic synthesis.¹ Various functional groups (ether, amine, amide, ester, etc.), called the directing group, are used to orientate the metalation. However, heavier element containing functional groups such as phosphine oxides or phosphonates can also be used.² For example, the use of ortho-lithiation on phosphine oxides can lead to the synthesis of original heterocycles such as the P, Si containing 6-membered ring **B** (Fig. 1).^{2d} Peri-Substitution is a double substitution in positions 1 and 8 of naphthalene (Nap) (or acenaphthene (Ace)) (Fig. 1b).³ Unique geometric constraints are imposed to the substituents connected to these positions, which are even closer than ortho-substitution. Such molecular engineering has been recently used to stabilize reactive species featuring main group elements (B, P, As etc.).⁴ Furthermore, the proximity between the peri-substituent offers the possibility of specific reactivity leading to the design original heterocycles such as P,Si heterocycle **D** (Fig. 1).^{5,6} During our study of multi-heteroatom-containing fluorophores,⁷ we noticed a specific reactivity of (8-bromonaphthalen-1-yl)diphenylphosphine oxide **E**⁸ with silanes: we observed a sequence of ortho and peri-lithiation followed by intramolecular cyclization of a nine-membered ring **F** (Fig. 1) through the formation of a disiloxane bridge. In this article, we present the straightforward synthesis of this unconventional heterocyclic platform, its reactivity, a detailed structural analysis and a study of its peculiar luminescent properties.

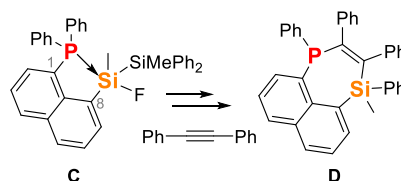
Literature

a) Ortho-lithiation toward the preparation of P,Si heterocycles



This work

b) Synthesis of peri-substituted P,Si heterocycles



c) Ortho- and peri-substitution toward the preparation of P,Si heterocycles

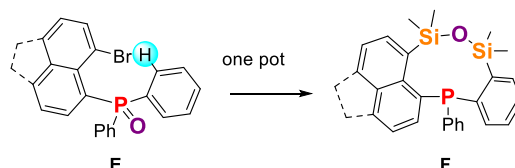
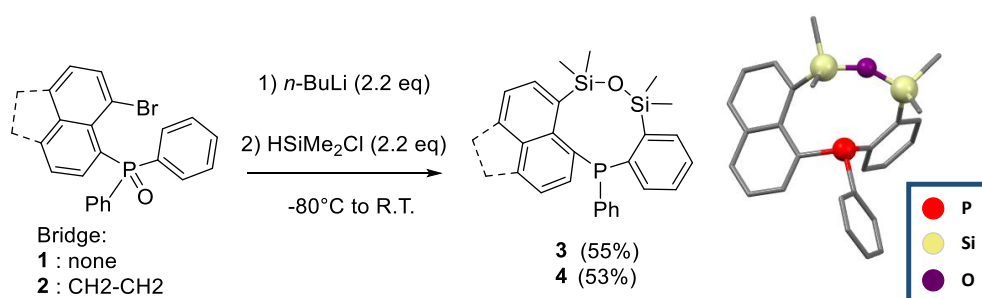


Fig.1: Example of ortho-substitution (a) and peri-substitution (b) toward the synthesis of P,Si heterocycles and strategy used in this work (c).

Results and discussion

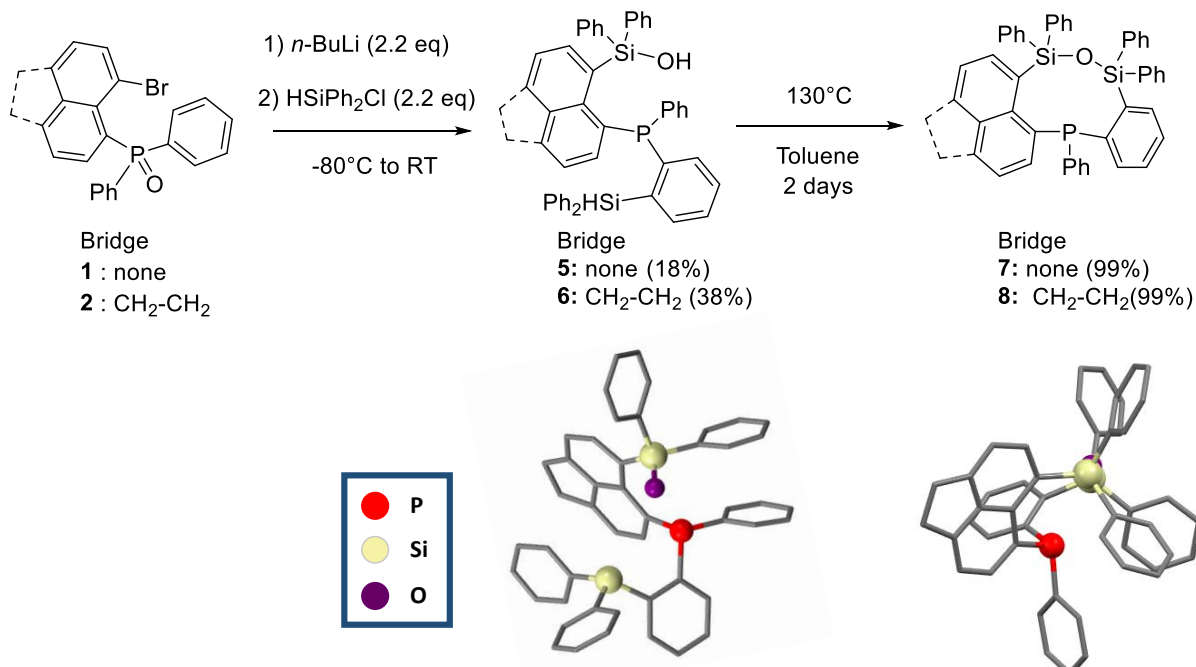
Synthesis

During our study of the reactivity of (8-bromonaphthalen-1-yl)diphenylphosphine oxide (Scheme 1),⁸ we observed that the lithiation of **1** followed by quenching with chlorodimethylsilane does not lead to the expected peri-substituted silane-phosphine oxide but to a peri-substituted Nap featuring a nine membered ring incorporating a phosphine and a disiloxane bridge (Compound **3**, Scheme 1). This unexpected compound was unambiguously characterized by multinuclear NMR, mass spectrometry and X-ray diffraction (Scheme 1, for full X-ray diffraction study and comparison, see below). At this point it is worth noting that during this sequence, a second Si-atom has been introduced in ortho-position of the P=O fragment and the P atom is reduced from σ^4, λ^5 -P to σ^3, λ^3 -P (see postulated mechanism below).⁹ Careful tuning of the reaction conditions (2.2 eq. of BuLi and HSiMe₂Cl) allowed to optimize the yield of **3** to 55%. Such synthetic method also efficiently works with Ace platform (**4**, Scheme 1).



Scheme 1: Synthesis of **3-4** and X-ray structure **3**

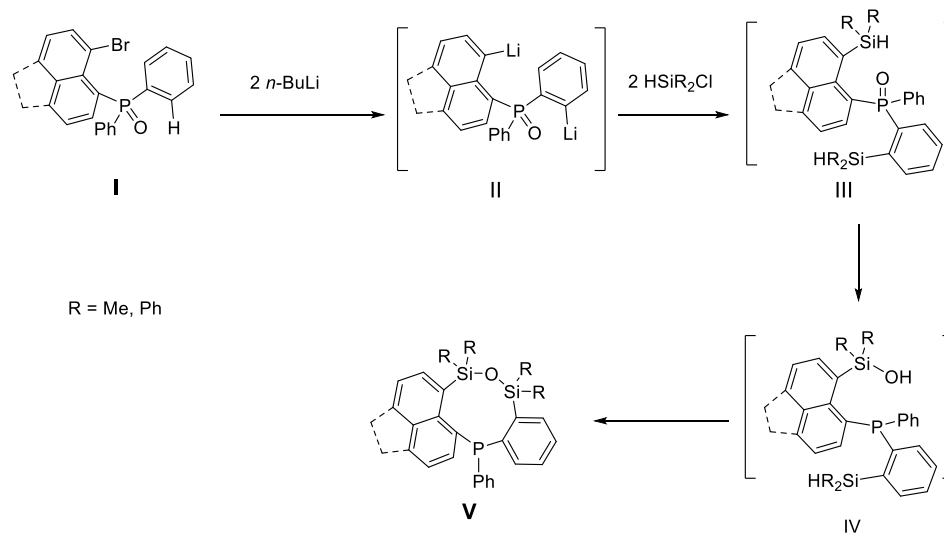
When bulkier diphenylchlorosilane is used as electrophile, the reaction stops at the silane-silanol intermediates **5-6** (Scheme 2) both with Nap and Ace platforms, probably due to the steric hindrance at the Si-atoms. In particular, the characterization of **6** (including X-ray diffraction, Scheme 2) unambiguously proves that the siloxane is formed on the peri-substituted Si-atom. The disiloxane formation could finally be obtained upon refluxing **5-6** in toluene to afford the cyclic derivatives **7-8**.



Scheme 2: Synthesis of **7-8** and X-ray structure of intermediate **6** and compound **8**

Such reaction pathway can be explained (Scheme 3). The 2.2 eq of BuLi allow performing the expected Li-halogen exchange but also an ortho-lithiation on the phenyl ring connected to the phosphine oxide (**II**, Scheme 3). Such

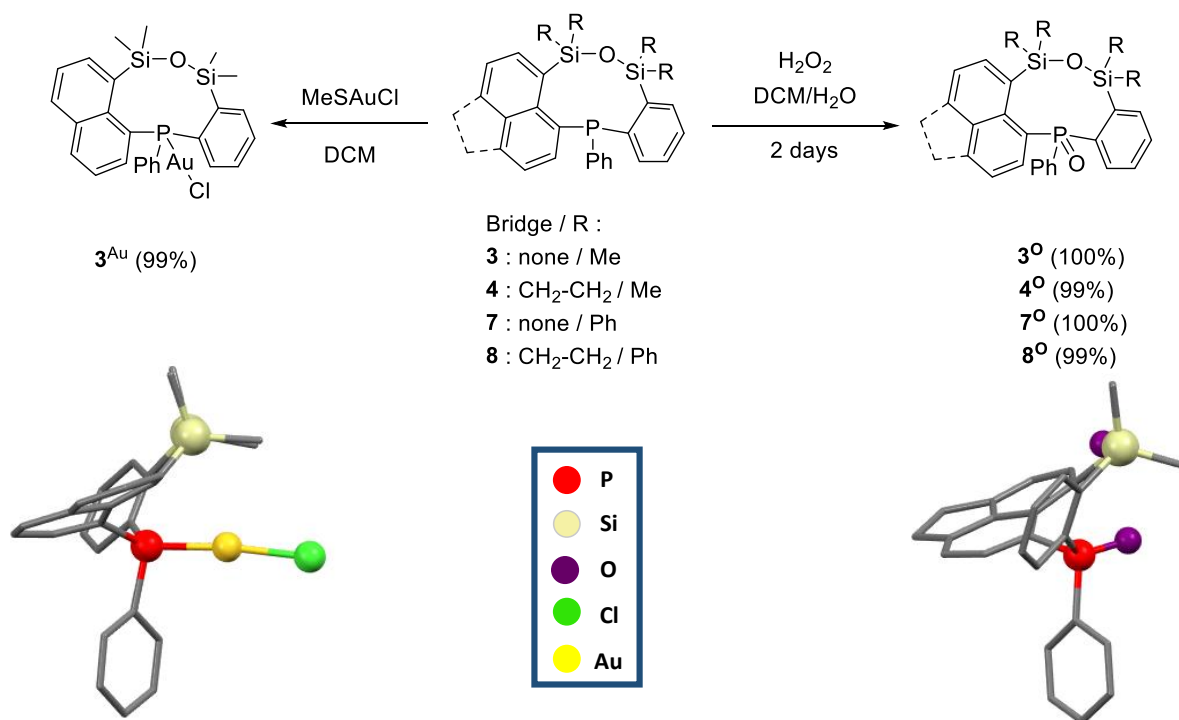
dilithiated derivatives is then quenched by chlorodimethylsilane to afford **III**. The phosphine oxide moiety of **III** was in situ deprotected by the peri-substituted silane function¹⁰ to afford the mixed silane-silanol derivatives **IV**. The fact that the reduction is performed by the peri-substituted silane is evidenced by the characterization of intermediate **6** (Scheme 2). Finally, the disiloxane bridge of **V** is formed in the last step, either spontaneously (**3,4**) or upon heating (**7,8**).



Scheme 3: postulated mechanism based on experimental observations

In short, a family of 4 cyclic phosphine-disiloxane featuring peri-substituted naphthyl scaffolds could be prepared in a very straightforward manner. They were all characterized by multinuclear NMR, mass spectrometry and X-ray diffraction. They display excellent air-stability both in solution and in solid, as well as good thermal stability ($T_{d_{10}}(\mathbf{4}) = 306^\circ\text{C}$).

Phosphines are known to display a rich reactivity toward oxidant, electrophile or metallic ions. However, the X-ray structures of **3,4** and **8** reveal that the lone pair of the P points toward the disiloxane bridge (Schemes 1,2), which can explain the excellent air stability of the compound. Nevertheless, the reactivity of the P-atom could be used and **3-4, 7-8** were quantitatively oxidized using H_2O_2 to afford **3^o**, **4^o**, **7^o** and **4^o** (scheme 4). Finally, the coordination ability these derivatives was evaluated using of **3** as prototype compound. The σ^3, λ^3 P-atom behaves as a classic two-electrons P-donor toward Au^{I} as evidenced by the formation of complex **3^{Au}** (Scheme 4).



Scheme 4: Synthesis 3^O - 4^O , 7^O - 8^O , 3^{Au} , X-ray structure of 4^O and 3^{Au}

In conclusion, a full family of 9 cyclic phosphine-disiloxane featuring peri-substituted naphthyl scaffolds have been prepared and fully characterized. The synthetic method allows introducing various naphthyl platforms (Nap and Ace), various Si substituents (Me and Ph). The P-atom remains reactive (oxidation, coordination) despite a highly sterically hindered scaffold.

Structural properties

Six of the nine compounds (**3**, **4**, 4^O , **8**, 8^O and 3^{Au}) could be crystallized and a full crystallographic data study and comparison within the family is thus possible (Table 1). A detailed inspection will be performed on **3**, then the general trend in the entire family will be discussed. **3** crystallizes in the P 21/c space group and the unit cell is composed by a racemic mixture of two enantiomers (the P atom in the molecule is stereogenic). The chemical structure of **3** is highly distorted due to the steric congestion to accommodate the trigonal P-atom, the 9-membered heterocycle and peri-substituents (Fig. 2). The P-C bond lengths and angles are classical for phosphane derivatives ($1.83 < d_{P-C} < 1.84$ Å), as well as the Si-C distances (1.90 Å $< d_{Si-C} < 1.92$ Å) et Si-O (1.63 Å $< d_{Si-O} < 1.64$ Å) (Table 1). The nine-membered ring display a boat-like conformation with equatorial position for the exocyclic P-Ph substituent (Figure 1c). Consequently, the P-lone pair points toward the disiloxane bridge and is sterically protected by the multiple substituent (see space fill, Fig. 2). The Si...P peri-distance in **3** (1, 3.189 Å, Table 1) is indicative for predominantly repulsive interactions, as previously observed by Beckmann *et al* on acyclic Ace peri-substituted with phosphine and silane.^{6a} Finally, the Nap is also distorted from planarity (Table 1) due to the presence of bulky substituent in peri-position. In the packing, π -dimers composed of the two enantiomers are observed in the solid-state (Fig. 4).

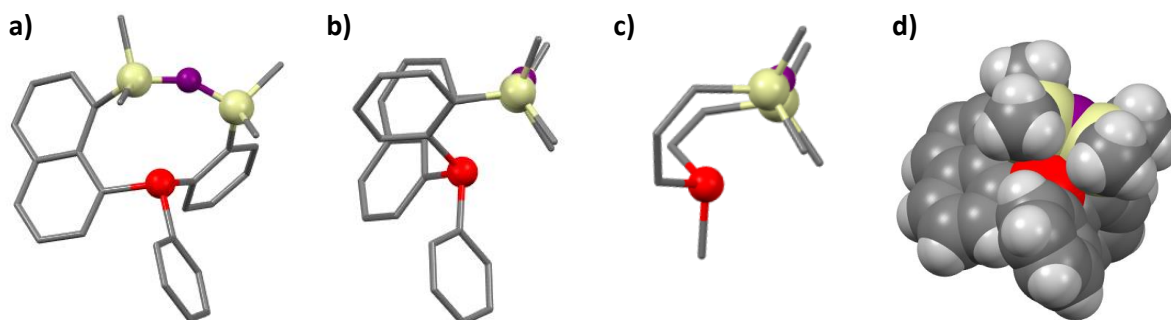


Fig. 2: (a, b) Different views of the crystallographic structure of **3**, (c) zoom on the 9-membered ring (substituents omitted for clarity) and (d) space fill representation of **3**

When Nap is replaced by Ace (**4**), most of the parameters remain valid (Table 1). Surprisingly, the presence of the Ph substituents on the Si in **8** has only a minor impact on the structural parameters (Fig. 3). Upon oxidation, the nine-membered ring shape is altered due to the repulsion between the P=O bond with the disiloxane bridge on one side, and the peri-substituted Si on the other one. Consequently, the P-Si peri distance increases as well as the distortion on the Nap/Ace platform (Fig. 3 and Table 1). Such observations are even more pronounced upon coordination of the Au^I (Fig. 3 and Table 1). Indeed, a stronger deformation is induced by the quasi-linear P-Au-Cl fragment (P-Au-Cl: 173.1°). In the packing, the effects of substituent are almost impossible to rationalize as Nap-Nap π -dimers are observed for **3** (Fig. 4), **4**, **8**, π -columns through Ace-Ace interactions for **4**^o (Fig. 4), while no clear interaction is found for **8**^o and **3**^{Au}.

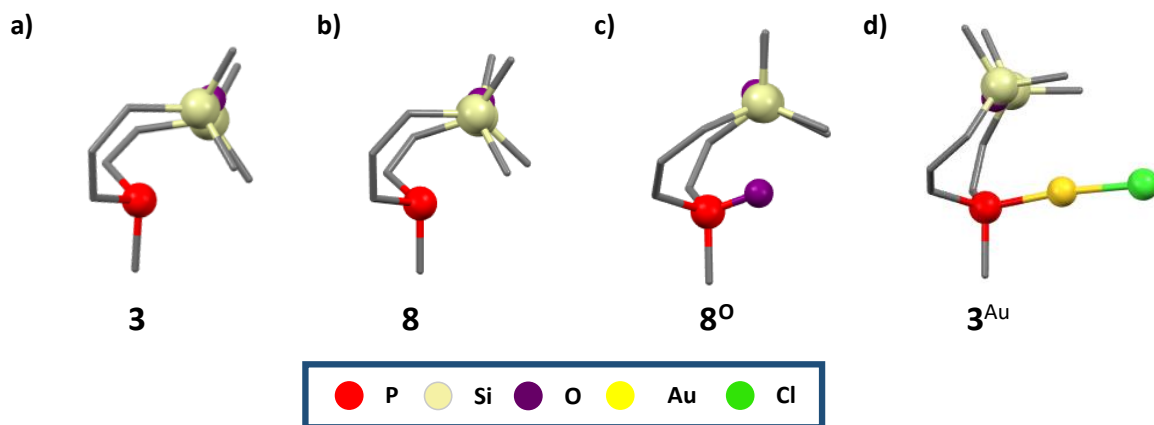


Fig. 3: Zooms on the 9-membered ring (substituents omitted for clarity) of (a) **3**, (b) **8**, (c) **8**^o and (d) **3**^{Au}

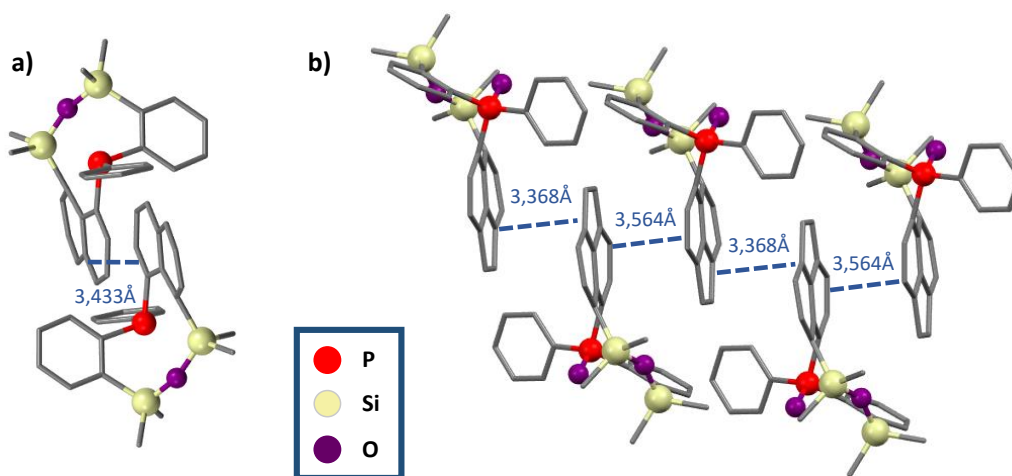


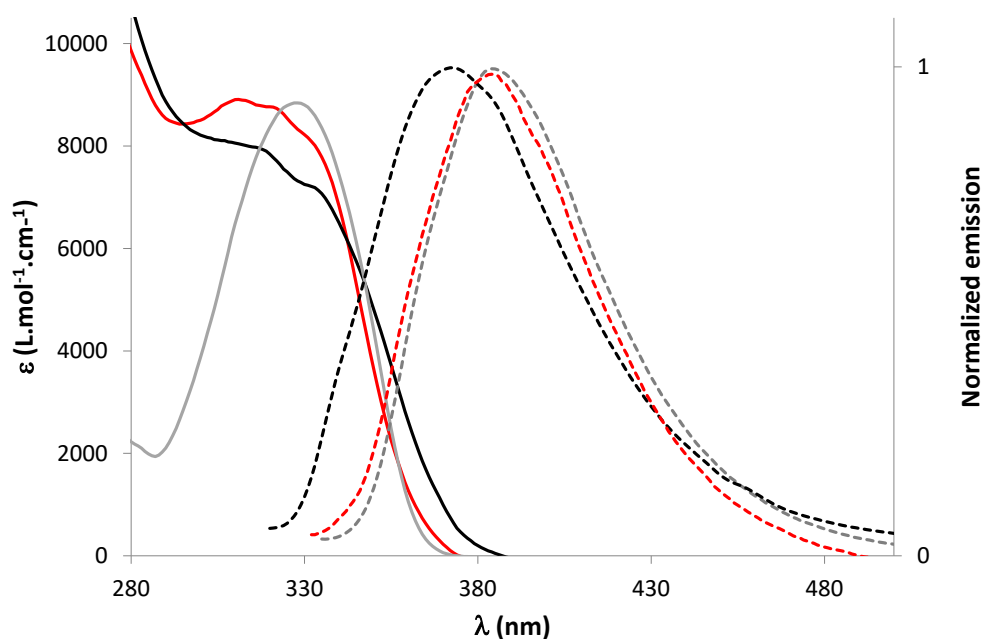
Fig. 4: Intermolecular interactions observed in the packing of (a) **3** and (b) **4**^o

Table 1: Crystallographic data

	3	4	8	4^o	8^o	3^{Au}
P-C ₁ (Å)	1.829(2)	1.835(2)	1.830(4)	1.811(2)	1.801(2)	1.821(8)
P-C ₅ (Å)	1.835(2)	1.839(1)	1.829(4)	1.817(3)	1.820(2)	1.829(7)
C ₁ -C ₂ (Å)	1.435(3)	1.445(2)	1.433(6)	1.441(4)	1.438(2)	1.440(1)
C ₂ -C ₃ (Å)	1.455(3)	1.452(2)	1.450(7)	1.439(4)	1.449(3)	1.440(1)
C ₃ -Si ₁ (Å)	1.921(2)	1.897(2)	1.878(5)	1.887(2)	1.893(2)	1.890(1)
Si ₁ -O (Å)	1.641(2)	1.639(1)	1.629(2)	1.632(2)	1.624(1)	1.642(5)
O-Si ₂ (Å)	1.637(2)	1.634(1)	1.625(3)	1.627(2)	1.624(1)	1.626(6)
Si ₂ -C ₄ (Å)	1.897(2)	1.890(1)	1.879(6)	1.886(3)	1.887(2)	1.886(9)
C ₄ -C ₅ (Å)	1.415(3)	1.410(2)	1.401(6)	1.414(3)	1.418(2)	1.410(1)
C ₁ -P-C ₅ (°)	103.00(1)	104.72(7)	101.00(2)	106.20(1)	105.50(8)	106.40(4)
<i>peri distances</i>						
P...Si	3.189	3.242	3.199	3.687	3.575	3.789

Optical properties

π -conjugated P-heterocycles and Si-heterocycles display rich optical properties,¹¹ the UV-vis absorption and fluorescence properties of **3-8** (resp **3^o -8^o**) were thus investigated in diluted dichloromethane (C = 10⁻⁵M) (table 2). They all display absorption bands in the UV characteristic of substituted Nap derivatives¹² and the effect of molecular engineering remain modest. For example, **4** displays absorptions bands with moderate extinction coefficient at λ_{max} (308 nm). The polyaromatic platform has a small influence on the absorption as the UV-vis absorption of the Ace derivatives is slightly red-shifted compared to their Nap analogues (Table 2 and Fig S19). The oxidation has the opposite effect as the σ^4, λ^5 -P-derivatives display a blue-shifted absorption compared to their σ^3, λ^3 -P-analogues (Table 2 and Fig 4). This can be explained by the stronger distortion of the π -system of the Nap/Ace induced by the presence of the P=O fragment (Table 2).

**Fig. 4:** Absorption (solid line) and emission (dotted line) spectra of **4** (red), **8** (black), **4^o** (grey) in diluted DCM

The fluorescent properties of the derivatives are more peculiar. While the P-trivalent derivatives featuring a Nap platform, are not luminescent in solution, all the other compounds display emission in the near UV, characteristic of substituted Nap/Ace derivatives.¹² Apart **4**^o, the luminescence quantum yields are modest (table 2). The effect of the substituents on the emission wavelength is also rather limited. While all the derivatives have modest luminescent properties in diluted solutions, crystalline samples of P-trivalent derivatives **3-4** and **7-8** display unexpected greenish luminescence (for example $\lambda_{em,solid}(\mathbf{4}) = 504$ nm while $\lambda_{em,liq}(\mathbf{4}) = 381$ nm) with quantum yields between 9% and 32% (Fig. 5 and Table 2). Such important red-shift of **3-4** and **7-8** is not observed for pentavalent P-derivatives which display weak solid-state luminescence in the spectral range of their emission in diluted solution (for example $\lambda_{em,solid}(\mathbf{4}^o) = 414$ nm while $\lambda_{em,liq}(\mathbf{4}^o) = 382$ nm, see Fig. S20). Such unexpected red-shifted solid-state emission can have two main origins: specific aggregate formation or triplet emission (phosphorescence).^{13,14} Time-resolved fluorescence measurements allowed to rule out the possibility of phosphorescence as all compounds display emission lifetime in the range of the ns, typical of fluorescent materials (see Figure S21-24). The study of the packing in the crystals did not allow to clarify the presence of specific interactions that would favour these observations, as some of these compounds form π -dimers but other don't. Finally, when the compound is isolated under the form of an amorphous material or diluted in PMA matrix (5% weight), no green luminescence could be observed, which clearly emphasizes the role of intermolecular interaction in the solid state, even if the inspection of X-Ray data did not allow to unravel their nature.

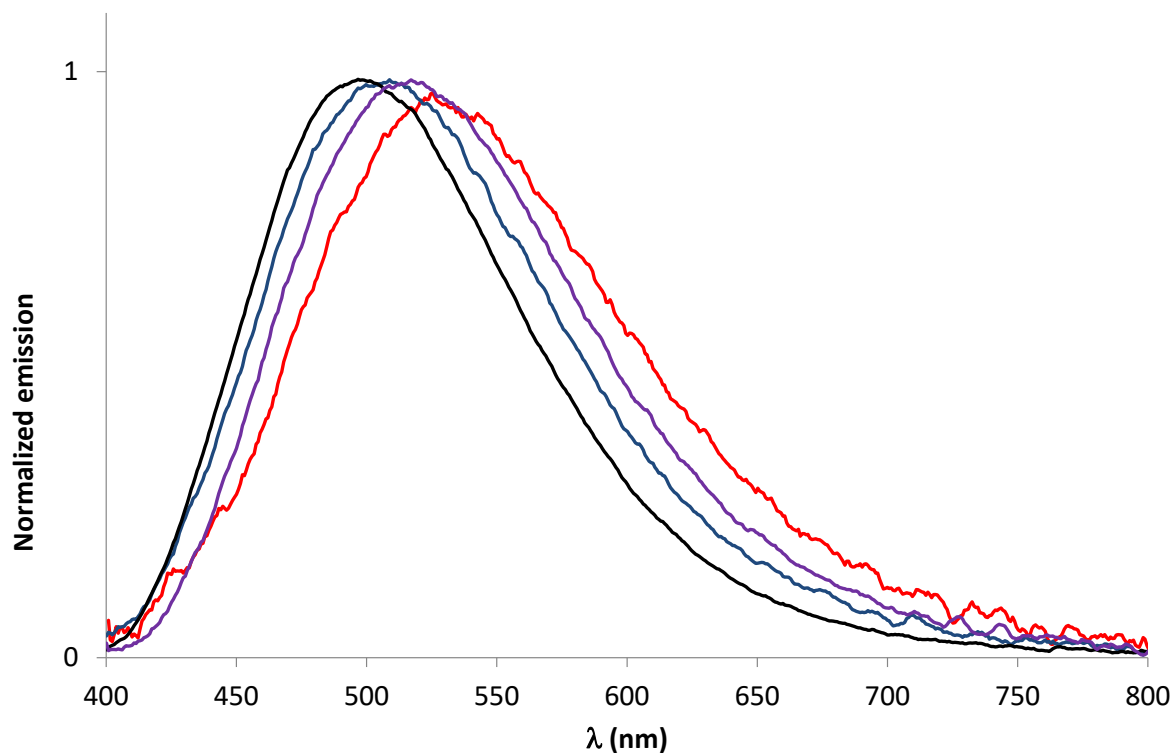


Fig. 5: Emission spectra in solid-state of **3**(blue), **4**(red), **7**(purple) and **8** (black)

Table 2: Photophysical data.

Compound	$\lambda_{\text{abs}}^{\text{a}}$ (nm)	ϵ_{max} (L.mol ⁻¹ .cm ⁻¹) ^a	λ_{0-0}^{a} (nm)	$\lambda_{\text{em}}^{\text{liq a}}$ (nm)	$\lambda_{\text{em}}^{\text{solid b}}$ (nm)	Stokes shift (cm ⁻¹) ^a	$\Phi_{\text{liquid}}^{\text{b}}$	$\Phi_{\text{solid}}^{\text{b}}$
3	322	7400	-	-	495	-	-	0.32
4	308	8900	350	381	504	6200	<0.01	0.09
7	327	7500	-	-	498	-	-	0.14
8	309	8000	345	371	495	5400	<0.01	0.11
3^o	310	7700	328	347	418	3400	0.07	0.07
4^o	327	8900	353	382	414	4400	0.60	0.08
7^o	309	8200	329	353	398	4000	0.05	0.05
8^o	322	8000	350	386	420	6600	0.06	0.01

^a Measured in diluted CH₂Cl₂ (10⁻⁵M). ^b Measured in calibrated integration sphere.

Conclusion

In conclusion, a full family of 9 cyclic phosphine-disiloxane featuring peri-substituted naphthyl and acenaphthyl scaffolds have been prepared and fully characterized. This straightforward synthesis takes advantage of both ortho- and peri-substitution of Nap/Ace-substituted phosphine oxides. The synthetic method allows introducing various polyaromatic platforms (Nap and Ace), various Si substituents (Me and Ph). Despite a strong steric congestion, the P-atom remains reactive (oxidation, coordination). In particular, Au(I) complex **3^{Au}** could be prepared. All the compounds display absorption/luminescence in the UV-vis. Surprisingly, the P-trivalent derivatives display unexpected green luminescence in the solid-state. Finally, given to their easy synthesis, these unconventional cyclic derivatives can be further used to design solid-state luminophore or cavity-shaped ligands for application in supramolecular catalysis.¹⁵

Acknowledgements

This work is supported by the Ministère de la Recherche et de l'Enseignement Supérieur, the CNRS, the Région Bretagne, the French National Research Agency (ANR Heterographene ANR-16-CE05-0003-01). Y. Molard, G. Taupier (Scanmat-UMS 2001) and C. Poriel (ISCR) are thanked for PLQY measurements.

Experimental section

General procedure. All experiments were performed under argon atmosphere using standard Schlenk techniques. Commercially available reagents were used as received without further purification. Solvents were freshly purified using MBRAUN SPS-800 drying columns. Separations were performed by gravity column chromatography on basic alumina (Aldrich, Type 5016A, 150 mesh, 58 Å) or silica gel (Merck Geduran 60, 0.063-0.200 mm). ¹H, ¹³C and ³¹P NMR spectra were recorded on a Bruker AV III 400 MHz NMR spectrometer equipped with BBFO probehead. Assignment of H and C atoms is based on COSY, NOESY, edited-HSQC and HMBC experiments. Special ³¹P decoupled experiments (³¹P-¹H, ³¹P-¹H/¹³C, ³¹P-HSQC, HMBC, COSY, NOESY) were performed on a Bruker Av III HD 500 MHz fitted with a triple inverse probehead (¹H-³¹P-X), part of the PRISM core facility (Biogenouest©, UMS Biosit, Université de Rennes 1- Campus de Villejean- 35043 RENNES Cedex, FRANCE). ¹H and ¹³C NMR chemical shifts were reported in parts per million (ppm) using residual solvent signal as reference (see ESI for nomenclature of NMR attribution). High-resolution mass spectra were obtained on a Varian MAT 311 or ZabSpec TOF Micromass instrument at CRMPO (Scanmat, UMS 2001). UV-Visible spectra were recorded rt on a VARIAN Cary 5000 spectrophotometer. The UV-Vis emission and excitation spectra measurements were recorded on a FL 920 Edinburgh Instrument equipped with a Hamamatsu R5509-73 photomultiplier for the NIR domain (300-1700 nm) and corrected for the response of the photomultiplier. The absolute quantum yields were measured with a C9920-03 Hamamatsu. Fluorescence decay measurements were carried out on the HORIBA Scientific Fluoromax - 4 equipped with its TCSPC pulsed source interface.

3: (General method A) 1^{16} (800 mg, 2.0 mmol, 1.0 eq) was dissolved in 40 mL of dry Et₂O. The solution was cooled down to -80°C then *n*-BuLi (1.92 mL, 4.4 mmol, 2.2 eq) was added dropwise and the solution was stirred for 30 mn at -80°C then 30 mn at room temperature (rt). The solution was again cooled down to -80°C and Me₂SiClH (416 mg, 4.4 mmol, 2.2 eq) was added dropwise. The mixture was then stirred at rt overnight. Then the solvent was evaporated and the crude was dissolved in DCM and extracted with water. The organic phase was dried over MgSO₄ and the solvent evaporated. The crude mixture was purified by silica gel chromatography using C₇/DCM (8/2), then recrystallized in C₇ to afford **3** as white crystals (390 mg, η = 44 %). ¹H NMR (400 MHz, CD₂Cl₂) δ 7.94(d, J = 1.1 Hz, 1H, H₃), 7.91 (d, J = 1.2 Hz, 1H, H₅), 7.87 (d, J = 1.2 Hz, 1H, H₁), 7.78-7.74 (m, 1H, H₇), 7.53-7.50 (m, 1H, H₈), 7.47 (t, J = 8.0 Hz, 1H, H₆), 7.45 (t, J = 6.9 Hz, 1H, H₂) 7.38-7.26 (m, 6H, H_{ortho, para, 9, 10, 11}), 7.09-7.04 (m, 2H, H_{meta}), 0.86 (d, J = 7.4 Hz, 3H, H_{Me}), 0.51 – 0.46 (m, 6H, H_{Me}), 0.28 (s, 3H, H_{Me}). ¹³C NMR (101 MHz, CD₂Cl₂) δ 147.5 (d, J_{C-P} = 43.3 Hz), 143.8 (d, J_{C-P} = 11.5 Hz), 141.3 (d, J_{C-P} = 33.7 Hz), 138.7 (d, J_{C-P} = 2.3 Hz), 138.6 (d, J_{C-P} = 3.0 Hz), 137.1 (d, J_{C-P} = 3.0 Hz), 136.8 (d, J_{C-P} = 13.1 Hz), 135.5 (d, J_{C-P} = 1.9 Hz), 134.7 (d, J_{C-P} = 7.8 Hz), 134.0 (d, J_{C-P} = 15.7 Hz), 133.7 (s), 132.7 (d, J_{C-P} = 17.6 Hz), 131.8 (s), 131.2 (d, J_{C-P} = 1.5 Hz), 129.8 (s), 128.8 (s), 128.7 (d, J_{C-P} = 5.1 Hz), 128.0 (s), 125.4 (s), 125.3 (s), 6.2 (d, J_{C-P} = 31.6 Hz, C_{Me}), 5.8 (s, C_{Me}), 3.4 (d, J_{C-P} = 6.0 Hz, C_{Me}), 0.77 (s, C_{Me}). ³¹P NMR (162 MHz, CD₂Cl₂) δ -20.9. HRMS (ASAP, 120°C) [M+H]⁺(C₂₆H₂₈OSi₂P) m/z Calculated : 443.1411 m/z, Found : 443.1410.

4: General method A was used with 2^{16} (1.00 g, 2.31 mmol, 1 eq), 20 mL of dry Et₂O, BuLi (2.21 mL, 5.08 mmol, 2.2 eq) and Me₂SiClH (481 mg, 5.08 mmol, 2.2 eq). The crude mixture was purified by silica gel chromatography (DCM/C₇ : 1/1), then recrystallized in C₇ to afford **4** as yellow crystals (650 mg, η = 60 %). ¹H NMR (400 MHz, CD₂Cl₂) δ 7.90 (d, 1H, J = 7.1 Hz), 7.85-7.83 (m, 1H), 7.61-7.57 (m, 1H), 7.50-7.47 (m, 1H), 7.33-7.26 (m, 7H), 7.22-7.18 (m, 2H), 3.35 (d, J = 3.6 Hz, 4H, H_{CH₂}), 0.75 (d, J = 6.7 Hz, 3H, H_{Me}), 0.55 (s, 3H, H_{Me}), 0.47 (d, J = 1.8 Hz, 3H, H_{Me}), 0.39 (s, 3H, H_{Me}). ¹³C NMR (101 MHz, CD₂Cl₂) δ 149.8 (s), 149.3 (d, J_{C-P} = 2.4 Hz), 148.3 (d, J_{C-P} = 47.7 Hz), 143.6 (d, J_{C-P} = 10.7 Hz), 139.6 (d, J_{C-P} = 33.3 Hz), 139.6 (d, J_{C-P} = 11.1 Hz), 138.3 (d, J_{C-P} = 2.0 Hz), 136.3 (d, J_{C-P} = 2.3 Hz), 133.6 (d, J_{C-P} = 15.7 Hz), 133.4 (d, J_{C-P} = 17.5 Hz), 132.7 (d, J_{C-P} = 9.5 Hz), 131.9 (d, J_{C-P} = 16.0 Hz), 131.8 (d, J_{C-P} = 16.3 Hz), 129.5 (s), 128.5 (d, J_{C-P} = 1.6 Hz), 128.1 (d, J_{C-P} = 4.3 Hz), 127.1 (s), 119.7 (s), 119.1 (s), 28.9 (d, J_{C-P} = 1.9 Hz, C_{CH₂}), 5.6 (d, J_{C-P} = 31.1 Hz, C_{Me}), 4.5 (s, C_{Me}), 3.1 (d, J_{C-P} = 9.2 Hz, C_{Me}), 0.2 (s, C_{Me}). 2 C are not observed due to overlap. ³¹P NMR (162 MHz, CD₂Cl₂) δ -24.2. HRMS (ASAP, 190°C) [M+H]⁺(C₂₈H₃₀O Si₂P) m/z Calculated : 469.1567, m/z Found : 469.1570.

5: General method A was used with compound **1** (500 mg, 1.2 mmol, 1 eq), 40 mL of dry Et₂O, *n*-BuLi (1.3 mL, 2.7 mmol, 2.2 eq) and Ph₂SiClH (592 mg, 2.7 mmol, 2.2 eq). The crude mixture was purified by silica gel chromatography (DCM/C₇ : 1/1) to afford **5** as a white powder (164 mg, η = 18 %). ¹H NMR (400 MHz, CD₂Cl₂) δ 7.94 (d, J = 8.0 Hz, 2H), 7.58 (d, J = 7.0 Hz, 1H), 7.44 – 7.38 (m, 4H), 7.37 – 7.11 (m, 23H), 7.06 (d, J = 7.6 Hz, 2H), 6.72 – 6.65 (m, 1H), 6.62 (t, J = 7.8 Hz, 2H), 6.12 (d, J = 25.2 Hz, 1H, H_{Si-OH}), 3.29 (d, J = 7.3 Hz, 1H, H_{Si-H}). ¹³C NMR (101 MHz, CD₂Cl₂) δ 143.9 (d, J_{C-P} = 8.7 Hz), 142.2 (d, J_{C-P} = 25.5 Hz), 141.9 (d, J_{C-P} = 17.1 Hz), 141.5, 138.4 (d, J_{C-P} = 5.0 Hz), 138.0 (d, J_{C-P} = 12.1 Hz), 137.8 (s), 137.6 (d, J_{C-P} = 13.5 Hz), 137.4 (s), 136.6 (s), 136.5 (s), 135.6 (s), 135.3 (s), 135.0 (s), 134.9 (s), 134.7 (d, J_{C-P} = 12.7 Hz), 133.6 (d, J_{C-P} = 17.1 Hz), 132.4 (d, J_{C-P} = 2.3 Hz), 132.2 (s), 131.2 (d, J_{C-P} = 8.8 Hz), 130.2 (s), 130.0 (d, J_{C-P} = 8.5 Hz), 129.6 (s), 129.3 (s), 128.8 – 128.6 (m), 128.4 (d, J_{C-P} = 12.1 Hz), 127.9 (s), 127.9 (s), 125.7 (d, J_{C-P} = 1.4 Hz), 125.3 (s). ³¹P NMR (162 MHz, CD₂Cl₂) δ -15.6. HRMS (ESI, CH₃COCH₃/CH₃OH : 95/5) [M-H]⁻(C₄₆H₃₆OSi₂P) m/z Calculated : 691.2048, m/z Found : 691.2052.

6 : General method B was used with **2** (400 mg, 0.924 mmol, 1 eq), 20 mL of dry Et₂O, *n*-BuLi (0.88 mL, 2.032 mmol, 2.2 eq) and Ph₂SiClH (445 mg, 2.032 mmol, 2.2 eq). The crude mixture was purified by silica gel chromatography (DCM/C₇: 1/1) to afford **6** as a white powder (253 mg, η = 38 %). ¹H NMR (300 MHz, CD₂Cl₂) δ 7.72 (d, J = 6.7 Hz, 1H), 7.53-7.45 (m, 3H), 7.43 – 7.36 (m, 3H), 7.36 – 7.26 (m, 5H), 7.26 – 7.06 (m, 14H), 7.04 – 6.92 (m, 4H), 6.82-6.71 (m, 3H), 5.90 (d, J = 3.5 Hz, 1H, H_{Si-OH}), 5.41 (d, J = 14.2 Hz, 1H, H_{Si-H}), 3.45 – 3.25 (m, 4H, H_{CH₂}). ¹³C NMR (101 MHz, CD₂Cl₂) δ 151.0 (d, J_{C-P} = 1.3 Hz), 150.7 (d, J_{C-P} = 2.2 Hz), 146.2 (d, J_{C-P} = 4.6 Hz), 143.3 (s), 141.2 (d, J_{C-P} = 32.4 Hz), 141.2 (d, J_{C-P} = 1.6 Hz), 140.5 (d, J_{C-P} = 9.6 Hz), 139.4 (s), 139.2 (d, J_{C-P} = 33.9 Hz), 138.4 (d, J_{C-P} = 4.9 Hz), 137.8 (d, J_{C-P} = 10.3 Hz), 136.2 (s), 136.0 (d, J_{C-P} = 21.4 Hz), 135.4 (d, J_{C-P} = 55.6 Hz), 134.2 (d, J_{C-P} = 2.5 Hz), 133.8 (d, J_{C-P} = 17.5 Hz), 133.3 (d, J = 3.0 Hz), 133.2 (d, J = 2.1 Hz), 130.1 (d, J = 1.5 Hz), 129.8 (d, J = 26.2 Hz), 129.4 (d, J_{C-P} = 6.1 Hz), 128.9 (d, J_{C-P} = 6.1 Hz), 128.6 (s), 128.1 (d, J_{C-P} = 26.9 Hz), 127.9 (s), 127.8 – 127.7 (m), 120.3 (d, J_{C-P} = 2.0 Hz), 119.3 (s), 30.3 (d, J_{C-P} = 3.3 Hz, C_{CH₂}). ³¹P NMR (121 MHz, CD₂Cl₂) δ -18.0. HRMS (ESI, CH₃COCH₃/CH₃OH : 95/5) [M-H]⁻(C₄₈H₃₈OSi₂P) m/z Calculated : 717.2204, m/z Found : 717.2197.

7 : **5** (119 mg, 0.172 mmol, 1 eq) was dissolved in dry toluene and the mixture heated during 48h to 130°C. After evaporation, **7** was recovered as a white powder (119 mg, η = 99 %). ¹H NMR (500 MHz, CD₂Cl₂) δ 7.90 (dd, J = 7.9, 1.6 Hz, 1H, H₅), 7.89 (dd, J = 8.2, 1.4 Hz, 1H, H₃), 7.77 (dd, J = 7.0, 1.4 Hz, 1H, H₁), 7.61 – 7.55 (m, 2H, SiPh), 7.54 (dd, J = 8.1, 1.5 Hz, 2H, SiPh), 7.57 – 7.50 (m, 2H, SiPh), 7.48 (dd, J = 7.1, 1.6 Hz, 1H, H₇), 7.49 – 7.42 (m, 1H, SiPh), 7.44 (t, J = 7.4 Hz, 1H, H₆), 7.40 – 7.33 (m, 2H, SiPh), 7.37 – 7.30 (m, 1H, SiPh), 7.36 – 7.29 (m, 1H, H₂), 7.34 – 7.27 (m, 1H, SiPh), 7.31 – 7.26 (m, 2H, H_{8,11}), 7.26-7.23 (m, 2H, SiPh), 7.23-7.20 (m, 2H, H_{9,para}), 7.20-7.18 (m, 2H, SiPh), 7.18-7.16 (d, J = 7.3 Hz, 1H, H₁₀), 7.16-7.15 (m, 2H, SiPh), 7.17 – 7.12 (m, 1H, SiPh), 7.12-7.08 (m, 2H, H_{meta}), 6.98 (t, J = 7.6 Hz, 2H, SiPh), 6.58 – 6.52 (m, 2H, H_{ortho}). ¹³C NMR (126 MHz, CD₂Cl₂) δ 144.2 (d, J_{C-P} = 49.1 Hz, C₁₃), 143.4 (d, J_{C-P} = 8.8 Hz, C₁₂), 142.8 (d, J_{C-P} = 19.7 Hz, C₂₁), 141.9 (d, J_{C-P} = 4.2 Hz, C₁), 141.7 (d, J_{C-P} = 1.9 Hz, C₁₇), 141.5 (d, J_{C-P} = 32.0 Hz, C₁₅), 138.3 (d, J_{C-P} = 10.2 Hz, C₁₄), 137.3 (d, J_{C-P} = 17.7 Hz, C₁₀), 137.2 (C₂₉), 136.7 (C₂₅), 136.2 (C₁₈), 136.0 (C₃₀), 135.9 (C₂₆), 135.08 (d, J = 8.8 Hz, C_{ipso}), 134.9 (C₁₁), 134.8 (C₄), 134.0 (C₇), 133.7 (d, J_{C-P} = 16.9 Hz, C₁₆), 132.8

(d, $J_{C-P} = 16.2$ Hz, C_{ortho}), 132.6 (d, $J_{C-P} = 4.2$ Hz, C_{22}), 132.3 (d, $J_{C-P} = 2.9$ Hz, C_3), 131.6 (C_5), 130.4 (C_8), 130.4 (C_{28}), 130.3 (C_{32}), 129.3 (d, $J_{C-P} = 1.6$ Hz, C_9), 129.2 (C_{20}), 128.5 (d, $J_{C-P} = 5.6$ Hz, C_{meta}), 128.4 (C_{para}), 128.2 (C_{31}), 128.2 (d, $J_{C-P} = 2.7$ Hz, C_{24}), 128.1 (C_{27}), 128.0 (C_{19}), 128.0 (m, C_{23}), 125.9 (s, C_6), 125.5 (s, C_2). ^{31}P NMR (162 MHz, CD_2Cl_2) δ -23.3. HRMS (ESI, CH_2Cl_2/CH_3OH : 90/10) $[M+Na]^+(C_{46}H_{35}ONaSi_2P)$ m/z Calculated : 713.1856, m/z Found : 713.1859.

8: 6 (160 mg, 0.223 mmol, 1 eq) was dissolved in dry toluene and the mixture was heated during 48h to 130°C. After evaporation, **8** was recovered as a white powder (160 mg, $\eta = 99\%$). 1H NMR (500 MHz, CD_2Cl_2) δ 7.65 (d, $J = 7.0$ Hz, 1H, H_1), 7.62 – 7.56 (m, 2H, H_{30}), 7.56 (dd, $J = 8.0, 1.4$ Hz, 2H, H_{18}), 7.56 (d, $J = 7.0$ Hz, 1H, H_7), 7.56 – 7.50 (m, 2H, H_{26}), 7.52 (d, $J = 7.3$ Hz, 1H, H_8), 7.46 (t, $J = 7.6$ Hz, 1H, H_{32}), 7.38 (t, $J = 7.3$ Hz, 2H, H_{31}), 7.36 – 7.33 (m, 2H, $H_{20,28}$), 7.37 – 7.27 (m, 1H, H_9), 7.30 (d, $J = 7.5$ Hz, 1H, H_6), 7.27 (t, $J = 7.2$ Hz, 2H, H_{19}), 7.22 – 7.18 (m, 3H, $H_{10,27}$), 7.18 – 7.16 (m, 2H, $H_{2,para}$), 7.13 (d, $J = 6.6$ Hz, 2H, H_{22}), 7.16 – 7.07 (m, 3H, $H_{11,meta}$), 7.08 (t, $J = 7.5$ Hz, 1H, H_{24}), 6.94 (t, $J = 7.6$ Hz, 2H, H_{23}), 6.75 – 6.71 (m, 2H, H_{ortho}), 3.44 – 3.29 (m, 4H, $H_{33,34}$). ^{13}C NMR (126 MHz, CD_2Cl_2) δ 150.9 (s, C_3), 150.1 (s, C_5), 144.7 (s, C_{13}), 144.5 (s, C_{12}), 143.2 (d, $J_{C-P} = 2.6$ Hz, C_1), 142.4 (d, $J_{C-P} = 17.2$ Hz, C_{21}), 140.9 (s, C_{17}), 140.3 (s, C_{15}), 140.2 (s, C_4), 137.5 (s, C_{29}), 137.3 (d, $J_{C-P} = 18.1$ Hz, C_{11}), 136.8 (d, $J_{C-P} = 1.6$ Hz, C_{25}), 136.7 (d, $J_{C-P} = 9.3$ Hz, C_{ipso}), 136.3 (s, C_{18}), 136.1 (s, C_{30}), 136.0 (s, C_{26}), 135.9 (s, C_7), 134.9 (s, C_8), 134.0 (s, C_{14}), 133.3 (d, $J_{C-P} = 4.0$ Hz, C_{22}), 132.5 (d, $J_{C-P} = 15.6$ Hz, C_{ortho}), 130.5 (s, C_9), 130.3 (s, C_{28}), 130.2 (s, C_{32}), 129.3 (s, C_{20}), 129.2 (s, C_{10}), 128.6 (d, $J_{C-P} = 1.5$ Hz, C_{16}), 128.3 (d, $J_{C-P} = 12.4$ Hz, C_{meta}), 128.2 (s, C_{24}), 128.2 (s, C_{31}), 128.0 (s, $C_{19,27}$), 127.9 (s, C_{para}), 127.8 (d, $J_{C-P} = 1.5$ Hz, C_{23}), 120.7 (s, C_6), 119.7 (s, C_2), 30.7 (s, C_{34}), 30.6 (s, C_{33}). ^{31}P NMR (121 MHz, CD_2Cl_2) -25.5. HRMS (ESI, CH_2Cl_2/CH_3OH : 90/10) $[M+Na]^+(C_{48}H_{37}ONaSi_2P)$ m/z Calculated : 739.2013, m/z Found : 739.2010.

3°: 3 (84 mg, 0.190 mmol, 1 eq) was dissolved in 10 ml of DCM. Then 2 ml of water and 0,08 mL of H_2O_2 (30%) were added. The mixture was stirred during 2 days at rt After evaporation, **3°** was recovered as a white powder (86 mg, $\eta = 99\%$). 1H NMR (400 MHz, CD_2Cl_2) δ 8.03 (d, $J = 8.0$ Hz, 1H), 7.87 (d, $J = 8.1$ Hz, 1H), 7.80 (d, $J = 7.3$ Hz, 2H), 7.62 – 7.51 (m, 3H), 7.48 – 7.30 (m, 4H), 7.28 – 7.21 (m, 2H), 6.95 – 6.84 (m, 2H), 0.87 (s, 3H, H_{Me}), 0.63 (s, 3H, H_{Me}), 0.39 (s, 3H, H_{Me}), 0.01 (s, 3H, H_{Me}). ^{13}C NMR (101 MHz, CD_2Cl_2) δ 146.5 (d, $J_{C-P} = 15.2$ Hz), 141.0 (s), 139.3 (d, $J_{C-P} = 102.1$ Hz), 137.3 (d, $J_{C-P} = 106.8$ Hz), 135.9 (s), 135.7 (d, $J_{C-P} = 14.2$ Hz), 134.2 (d, $J_{C-P} = 9.2$ Hz), 133.9 (d, $J_{C-P} = 3.5$ Hz), 133.9 (s), 133.8 (d, $J_{C-P} = 1.9$ Hz), 132.1 (d, $J_{C-P} = 8.9$ Hz), 131.3 (d, $J_{C-P} = 2.7$ Hz), 130.9 (d, $J_{C-P} = 2.9$ Hz), 129.6 (s), 128.5 (d, $J_{C-P} = 11.9$ Hz), 128.3 (s), 125.8 (s), 123.3 (d, $J_{C-P} = 15.4$ Hz) 7.3 (s, C_{Me}), 4.0 (s, C_{Me}), 3.9 (d, $J = 2.0$ Hz, C_{Me}), 1.7 (s, C_{Me}). ^{31}P NMR (162 MHz, CD_2Cl_2) δ +34.8. HRMS (ESI, CH_2Cl_2/CH_3OH : 90/10) $[M+K]^+(C_{26}H_{27}O_2Si_2PK)$ m/z Calculated : 497.0919, m/z Found : 497.0920.

4° :4 (98 mg, 0.209 mmol, 1 eq) was dissolved in 10 ml of DCM. Then 2 ml of water and 0.08 ml of H_2O_2 (30%) were added. The mixture was stirred during 2 days at r.t. The mixture was stirred during 2 days at rt and then extracted with water. The solvent was finally evaporated to afford **4°** as a white powder (100 mg, $\eta = 99\%$). 1H NMR (400 MHz, CD_2Cl_2) δ 7.80 (d, $J = 7.0$ Hz, 1H), 7.78 – 7.75 (m, 1H), 7.63 (dd, $J = 16.3, 7.2$ Hz, 1H), 7.56 – 7.47 (m, 2H), 7.45 – 7.37 (m, 3H), 7.32 – 7.25 (m, 3H), 7.10 – 7.03 (m, 2H), 3.52 – 3.31 (m, 4H), 0.78 (s, 3H, H_{Me}), 0.61 (s, 3H, H_{Me}), 0.39 (s, 3H, H_{Me}), 0.12 (s, 3H, H_{Me}). ^{13}C NMR (101 MHz, CD_2Cl_2) δ 153.1 (d, $J_{C-P} = 3.3$ Hz), 148.3 (d, $J_{C-P} = 1.5$ Hz), 146.6 (d, $J_{C-P} = 15.1$ Hz), 140.6 (s), 139.8 (d, $J_{C-P} = 10.4$ Hz), 139.4 (d, $J_{C-P} = 42.4$ Hz), 138.7, 138.15 (s), 136.5 (d, $J_{C-P} = 13.5$ Hz), 135.9 (d, $J_{C-P} = 7.2$ Hz), 135.6 (d, $J_{C-P} = 14.1$ Hz), 133.4 (d, $J_{C-P} = 14.0$ Hz), 132.2 (d, $J_{C-P} = 9.3$ Hz), 131.2 (d, $J_{C-P} = 2.7$ Hz), 130.7 (d, $J_{C-P} = 3.0$ Hz), 128.5 (d, $J_{C-P} = 12.2$ Hz), 128.4 (d, $J_{C-P} = 11.6$ Hz), 122.6 (d, $J_{C-P} = 102.9$ Hz), 120.0 (s), 117.6 (d, $J_{C-P} = 15.2$ Hz), 30.6 (d, $J_{C-P} = 1.4$ Hz), 30.4 (s, C_{CH_2}), 7.3 (s, C_{Me}), 4.5 (d, $J_{C-P} = 2.0$ Hz, C_{Me}), 4.1 (s, C_{Me}), 1.9 (s, C_{Me}). ^{31}P NMR (162 MHz, CD_2Cl_2) δ +35.2. HRMS (ESI, CH_3COCH_3/CH_3OH : 9/1) $[M+H]^+(C_{28}H_{30}O_2Si_2P)$ m/z Calculated : 485.1517, m/z Found : 485.1519.

7° :7 (70 mg, 0.101 mmol, 1 eq) was dissolved in 10 ml of DCM. Then 2 ml of water and 0.08 ml of H_2O_2 (30%) were added. The mixture was stirred during 2 days at r.t. The solution was extracted with water and then the solvent was evaporated to afford **7°** as a white powder (71 mg, $\eta = 100\%$). 1H NMR (400 MHz, CD_2Cl_2) δ 8.09 (d, $J = 7.7, 1.8$ Hz, 1H, H_5), 7.89 (d, $J = 8.1, 1.6$ Hz, 1H, H_3), 7.77 (d, $J = 6.9, 1.2$ Hz, 1H, H_1), 7.70 – 7.65 (m, 1H, H_{11}), 7.57 – 7.51 (m, 5H, $H_{7,26,30}$), 7.51 – 7.23 (m, 15H, $H_{2,6,8,9,10,22,24,28,31,32,meta,para}$), 7.17 – 7.10 (m, 6H, $H_{23,27,ortho}$), 7.10 – 7.06 (m, 1H, H_{20}), 6.96 – 6.90 (m, 2H, H_{19}), 6.89 – 6.85 (m, 2H, H_{18}). ^{13}C NMR (126 MHz, CD_2Cl_2) δ 145.0 (s, C_{17}), 141.9 (d, $J_{C-P} = 15.1$ Hz, C_{12}), 140.5 (d, $J_{C-P} = 101.6$ Hz, C_{13}), 139.1 (s, $C_{1,25}$), 138.3 (d, $J_{C-P} = 13.9$ Hz, C_{11}), 137.1 (s, C_{21}), 137.1 (d, $J_{C-P} = 5.5$ Hz, C_{15}), 136.4 (s, C_{29}), 136.3 (s, C_{30}), 136.1 (d, $J_{C-P} = 3.2$ Hz, C_{43}), 135.6 (s, C_{22}), 135.5 (s, C_{26}), 135.4 (s, C_{18}), 135.1 (d, $J_{C-P} = 102.4$ Hz, C_{ipso}), 134.4 (d, $J_{C-P} = 3.5$ Hz, C_5), 134.3 (d, $J_{C-P} = 9.3$ Hz, C_4), 133.9 (d, $J_{C-P} = 12.0$ Hz, C_7), 133.8 (d, $J_{C-P} = 14.2$ Hz, C_8), 132.5 (d, $J_{C-P} = 8.6$ Hz, C_{ortho}), 131.6 (d, $J_{C-P} = 2.8$ Hz, C_{para}), 130.7 (d, $J_{C-P} = 2.9$ Hz, C_{10}), 130.4 (s, C_{28}), 130.1 (s, C_3), 129.8 (s, C_{24}), 128.7 (d, $J_{C-P} = 12.4$ Hz, C_9), 128.6 (d, $J_{C-P} = 11.8$ Hz, C_{metha}), 128.5 (s, C_{32}), 128.3 (s, C_{20}), 128.0 (s, C_{31}), 127.8 (s, C_{23}), 127.2 (d, $J_{C-P} = 101.8$ Hz, C_{14}), 127.2 (s, C_{19}), 127.1 (s, C_{27}), 125.5 (s, C_2), 123.8 (d, $J_{C-P} = 15.3$ Hz, C_6). ^{31}P NMR (162 MHz, CD_2Cl_2) δ +33.6. HRMS (ESI, CH_2Cl_2/CH_3OH : 90/10) $[M+H]^+(C_{46}H_{35}O_2Si_2P)$ m/z Calculated : 707.1986, m/z Found : 707.1983.

8°: 8 (41 mg, 0.057 mmol, 1 eq) was dissolved in 6 ml of DCM. Then 1 ml of water and 0,04 ml of H_2O_2 (30%) (0,08 mL, 0.190 mmol, 4 eq) was added. The mixture was stirred during 2 days at rt The solution was extracted with water and then the solvent was evaporated to afford **8°** as a white powder (42 mg, $\eta = 100\%$). 1H NMR (400 MHz, CD_2Cl_2) δ 7.77 (d, $J = 7.1$ Hz, 1H, H_1), 7.64 (dd, $J = 16.2, 7.1$ Hz, 1H, H_7), 7.52 – 7.30 (m, 18H, $H_{6,8,9,10,11,22,26,28,30,32,ortho,meta,para}$), 7.26 – 7.15 (m, 9H, $H_{2,18,20,24,27,31}$), 7.10 – 7.03 (m, 4H, $H_{19,23}$), 3.51 – 3.38 (m, 4H, $H_{33,34}$). ^{13}C NMR (126 MHz, CD_2Cl_2) δ 153.8 (d, $J_{C-P} = 2.9$ Hz, C_5),

149.5 (s, C₃), 145.6 (s, C₁₇), 143.3 (s, C₁), 142.2 (d, J_{C-P} = 14.7 Hz, C₁₂), 141.1 (s, C₂₁), 140.3 (d, J_{C-P} = 100.9 Hz, C₁₃), 140.1 (d, J_{C-P} = 10.8 Hz, C₄), 138.9 (s, C₂₅), 138.8 (d, J_{C-P} = 14.1 Hz, C₉), 137.6 (s, C₂₉), 137.5 (d, J_{C-P} = 7.5 Hz, C₁₅), 136.4 (d, J_{C-P} = 13.5 Hz, C₇), 136.1 (s, C₂₆), 136.0 (s, C₁₈), 135.9 (s, C₃₀), 135.8 (d, J_{C-P} = 105.6 Hz, C_{ipso}), 134.9 (s, C₂₂), 133.2 (d, J_{C-P} = 13.5 Hz, C₈), 132.5 (d, J_{C-P} = 9.3 Hz, C_{ortho}), 131.7 (d, J_{C-P} = 2.7 Hz, C_{para}), 130.5 (d, J_{C-P} = 3.0 Hz, C₁₀), 130.2 (d, J_{C-P} = 2.2 Hz, C₁₆), 129.7 (s, C₃₂), 129.5 (s, C₂₈), 129.0 (d, J_{C-P} = 12.2 Hz, C₁₁), 128.7 (d, J_{C-P} = 11.8 Hz, C_{meta}), 128.2 (s, C₂₀), 128.0 (s, C₂₄), 127.7 (s, C₂₇), 127.7 (s, C₃₁), 127.2 (s, C₁₉), 126.9 (s, C₂₃), 123.4 (d, J_{C-P} = 102.6 Hz, C₁₄), 119.9 (s, C₂), 118.3 (d, J_{C-P} = 15.1 Hz, C₆), 30.7 (s, C₃₃), 30.4 (s, C₃₄). ³¹P NMR (162 MHz, CD₂Cl₂) δ +34.0. HRMS (ESI, CH₃OH/CH₂Cl₂ : 90/10) [M+Na]⁺(C₄₈H₃₇O₂NaSi₂P) m/z Calculated : 755.1962, m/z Found : 755.1968.

3^{Au}: **3** (70 mg, 0.158 mmol, 1 eq) and Me₂SAuCl (47 mg, 0.158 mmol, 1 eq) were dissolved in 8 mL of DCM and the reaction was stirred overnight. Then, the mixture was filtered on celite and the solvent removed to afford **3AuCl** as a white powder (105 mg, η = 99 %). ¹H NMR (400 MHz, CD₂Cl₂) δ 8.09 (d, J = 8.0, 1H), 7.92 (d, J = 8.2, 1H), 7.85 (d, J = 6.7, 1.2 Hz, 1H), 7.79 – 7.70 (m, 2H), 7.62 – 7.43 (m, 5H), 7.31 – 7.24 (m, 1H), 7.24 – 7.16 (m, 2H), 6.52 (t, J = 9.9 Hz, 2H), 1.11 (s, 3H, H_{Me}), 0.88 (s, 3H, H_{Me}), 0.37 (s, 3H, H_{Me}), -0.37 (s, 3H, H_{Me}). ¹³C NMR (101 MHz, CD₂Cl₂) δ 145.8 (d, J_{C-P} = 22.8 Hz), 138.4 (d, J_{C-P} = 12.3 Hz), 138.3 (d, J_{C-P} = 4.6 Hz), 136.8 (d, J_{C-P} = 26.3 Hz), 136.6 (d, J_{C-P} = 3.6 Hz), 136.3 (d, J_{C-P} = 25.2 Hz), 135.7 (d, J_{C-P} = 9.4 Hz), 135.6 (d, J_{C-P} = 5.6 Hz), 134.8 (d, J_{C-P} = 7.6 Hz), 134.6 (d, J_{C-P} = 8.8 Hz), 133.9 (d, J_{C-P} = 3.2 Hz), 132.9 (d, J_{C-P} = 12.7 Hz), 130.7 (d, J_{C-P} = 2.9 Hz), 130.3 (d, J_{C-P} = 1.9 Hz), 130.3 (d, J_{C-P} = 2.2 Hz), 129.6 (d, J_{C-P} = 9.2 Hz), 128.7 (d, J_{C-P} = 10.5 Hz), 126.8, 126.6 (d, J_{C-P} = 63.3 Hz), 124.9 (d, J_{C-P} = 10.6 Hz), 5.7 (C_{Me}), 3.8 (C_{Me}), 2.2 (C_{Me}), 2.0 (C_{Me}). ³¹P NMR (162 MHz, CD₂Cl₂) δ +25.4. HRMS (ESI, CH₂Cl₂/CH₃OH: 90/10) [M+Na]⁺(C₂₆H₂₇O³⁵ClNaSi₂PAu) m/z Calculated : 697.0584, m/z Found : 697.0589.

¹ M. C. Whisler, S. MacNeil, V. Snieckus and P. Beak, Beyond Thermodynamic Acidity: A Perspective on the Complex-Induced Proximity Effect (CIPE) in Deprotonation Reactions, *Angew. Chem. Int. Ed.*, 2004, **43**, 2206-2225.

² a) B. Schaub, T. Jenny and M. Schlosser, Ortho-lithiation of triphenylphosphonio-methylid and, also, triphenylphosphine oxide, *Tetrahedron Lett.*, 1984, **25**, 4097-4100; b) W. Michael and M. Kurt, Metallation Reactions on 2,20 - Bis(diphenylphosphinoyl)-1,10 -binaphthyl [BINAP(O)₂] *Bull. Chem. Soc. Jap*, 2003, **76**, 1233-1244; c) M. A. del Águila-Sánchez, Y. Navarro, J. García López, G. P. Guedes and F. López Ortiz, Synthesis of P-stereogenic diarylphosphinic amides by directed lithiation: transformation into tertiary phosphine oxides *via* methanolysis, aryne chemistry and complexation behaviour toward zinc(II), *Dalt. Trans.*, 2016, **45**, 2008-2022. d) H. Tsuji, S. Komatsu, Y. Kanda, T. Umehara, T. Saeki and K. Tamao, Double Ortho-lithiation of Diethylamino diphenylphosphine Oxide and *tert*-Butyldiphenylphosphine Oxide, *Chem. Lett.*, 2006, **35**, 758-759.

³ P. Kilian, F. R. Knight and J. D. Woollins, Naphthalene and Related Systems *peri*-Substituted by Group 15 and 16 Elements, *Chem. Eur. J.*, 2011, **17**, 2302-2328.

⁴ a) B. A. Chalmers, M. Bühl, K. S. Athukorala Arachchige, A. M. Z. Slawin and P. Kilian, Geometrically Enforced Donor-Facilitated Dehydrocoupling Leading to an Isolable Arsanylidine-Phosphorane, *J. Am. Chem. Soc.*, 2014, **136**, 6247-6250. b) B. A. Surgenor, M. Bühl, A. M. Z. Slawin, J. D. Woollins and P. Kilian, Isolable Phosphanylidene Phosphorane with a Sterically Accessible Two-Coordinate Phosphorus Atom, *Angew. Chem. Int. Ed.*, 2012, **51**, 10150-10153. c) M. Devillard, R. Brousses, K. Miqueu, G. Bouhadir and D. Bourissou, A Stable but Highly Reactive Phosphine-Coordinated Borenium: Metal-free Dihydrogen Activation and Alkyne 1,2-Carboboration *Angew. Chem. Int. Ed.*, 2015, **54**, 5722-5726. d) A. J. Rosenthal, M. Devillard, K. Miqueu, G. Bouhadir and D. Bourissou, A Phosphine-Coordinated Boron-Centered Gomberg-Type Radical, *Angew. Chem. Int. Ed.*, 2015, **54**, 9198-9202. e) M. Olaru, R. Kather, E. Hupf, E. Lork, S. Mebs and J. Beckmann, A Monoaryllead Trichloride That Resists Reductive Elimination, *Angew. Chem. Int. Ed.*, 2018, **57**, 5917-5920.

⁵ A. Toshimitsu, T. Saeki and K. Tamao, Phosphonium Sila-ylide: Reaction Pathway Different from Ammonium Sila-ylide but Similar to Phosphonium Ylide *J. Am. Chem. Soc.*, 2001, **123**, 9210-9211.

⁶ For other P,Si *peri*-substituted Ace see: a) E. Hupf, E. Lork, S. Mebs and J. Beckmann, Sterically Congested 5-Diphenylphosphinoacenaphth-6-yl-silanes and -silanols, *Organometallics*, 2015, **34**, 3873-3887; b) E. Hupf, M. Olaru, C. I. Raț, M. Fugel, C. B. Hübschle, E. Lork, S. Grabowsky, S. Mebs and J. Beckmann, Mapping the Trajectory of Nucleophilic Substitution at Silicon Using a *peri*-Substituted Acenaphthyl Scaffold *Chem. Eur. J*, 2017, **23**, 10568-10579; c) E. Hupf, L. A. Malaspina, S. Holsten, F. Kleemiss, A. J. Edwards, J. R. Price, V. Kozich, K. Heyne, S. Mebs, S. Grabowsky and J. Beckmann, Proximity Enforced Agostic Interactions Involving Closed-Shell Coinage Metal Ions, *Inorg. Chem.*, 2019, **58**, 16372-16378; d) S. Holsten, E. Hupf, E. Lork, S. Mebs and J. Beckmann, Proximity enforced oxidative addition of a strong unpolar σ-Si-Si bond at rhodium(I) *Dalton Trans.*, 2020, **49**, 1731-1735.

⁷ a) H. Chen, W. Delaunay, J. Li, Z. Wang, P.-A. Bouit, D. Tondelier, B. Geffroy, F. Mathey, Z. Duan, R. Réau and M. Hissler, Benzofuran-fused Phosphole: Synthesis, Electronic, and Electroluminescence Properties, *Org. Lett.*, 2013, **15**, 330-333. b) H. Chen, M. Denis, P.-A. Bouit, Y. Zhang, X. Wei, D. Tondelier, B. Geffroy, Z. Duan and M. Hissler, Blue Electrofluorescence Properties of Furan-Silole Ladder Pi-Conjugated Systems, *Applied Sciences*, 2018, **8**, 812. c) T. Delouche, A. Mocanu, T.

-
- Roisnel, R. Szűcs, E. Jacques, Z. Benkő, L. Nyulászi, P.-A. Bouit and M. Hissler, π -Extended Phosphepines: Redox and Optically Active P-Heterocycles with Nonplanar Framework, *Org. Lett.*, 2019, **21**, 802-806.
- ⁸ T. Delouche, R. Mokrai, T. Roisnel, D. Tondelier, B. Geffroy, L. Nyulászi, Z. Benkő, M. Hissler and P.-A. Bouit, Naphthyl-Fused Phosphepines: Luminescent Contorted Polycyclic P-Heterocycles, *Chem. Eur. J.*, 2020, **26**, 1856-1863.
- ⁹ σ represents the coordination number and λ the valence of the P-atom
- ¹⁰ E. Podyacheva, E. Kuchuk and D. Chusov, Reduction of phosphine oxides to phosphines, *Tetrahedron Lett.*, 2019, **60**, 575-582.
- ¹¹ a) T. Baumgartner, F. Jaekle, (Eds), Main Group Strategies toward Functional Hybrid Materials, **2018**, John Wiley & Sons (UK); b) M. Hissler, P. W. Dyer and R. Réau, Linear organic pi-conjugated systems featuring the heavy Group 14 and 15 elements *Coord. Chem. Rev.*, 2003, **244**, 1-44; c) D. Joly, P. A. Bouit and M. Hissler, Organophosphorus derivatives for electronic devices, *J. Mater. Chem. C*, 2016, **4**, 3686-3698.
- ¹² H. Maeda, T. Maeda, K. Mizuno, Absorption and Fluorescence Spectroscopic Properties of 1- and 1,4-Silyl-Substituted Naphthalene Derivatives *Molecules* 2012, **17**, 5108-5125
- ¹³ M. Baroncini, G. Bergamini and P. Ceroni, Rigidification or interaction-induced phosphorescence of organic molecules, *Chem. Commun.*, 2017, **53**, 2081-2093.
- ¹⁴ For specific example of P,O,Si containing p-systems featuring room temperature phosphorescence see: M. Shimizu, S. Nagano and T. Kinoshita, Dual Emission from Precious Metal-Free Luminophores Consisting of C, H, O, Si, and S/P at Room Temperature *Chem. Eur. J.*, 2020, **26**, 5162-5167.
- ¹⁵ a) D. Sémeril and D. Matt, Synthesis and catalytic relevance of P(III) and P(V)-functionalised calixarenes and resorcinarenes *Coord. Chem. Rev.* **2014**, 279, 58-95b) F. Elaieb, D. Sémeril, D. Matt, M. Pfeffer, P.-A. Bouit, M. Hissler, C. Gourlaouen and J. Harrowfield, Calix[4]arene-fused phospholes, *Dalton Trans.*, 2017, **46**, 9833-9845.
- ¹⁶ J. Beckmann, T. Giang Do, S. Grabowsky, E. Hupf, E. Lork and S. Mebs Peri-Interactions in 8-Diphenylphosphino-1-bromonaphthalene, 6-Diphenylphosphino-5-bromoacenaphthene, and Derivatives, *Z. Anorg. Allg. Chem.* **2013**, 2233-2249